Bond Strengths of Transition Metal Diatomics: Zr_2, YCo, YNi, ZrCo, ZrNi, NbCo, and NbNi

Caleb A. Arrington, Thorsten Blume, and Michael D. Morse*

Department of Chemistry, University of Utah, Salt Lake City, Utah 84112

Mats Doverstål and Ulf Sassenberg

Department of Physics, Stockholm University, Vanadisvägen 9, 11346 Stockholm, Sweden

Received: September 27, 1993; In Final Form: November 28, 1993®

The observation of an abrupt predissociation threshold in an extremely congested electronic spectrum has been used to measure the bond dissociation energies of the mixed early–late transition metal molecules YCo, YNi, ZrCo, ZrNi, NbCo, and NbNi. In these systems it is argued that predissociation occurs as soon as the ground separated atom limit is exceeded, providing values of D_0°(YCo) = 2.591 ± 0.001 eV, D_0°(YNi) = 2.904 ± 0.001 eV, D_0°(ZrCo) = 3.137 ± 0.001 eV, D_0°(ZrNi) = 2.861 ± 0.001 eV, D_0°(NbCo) = 2.729 ± 0.001 eV, and D_0°(NbNi) = 2.780 ± 0.001 eV. In addition, the bond strength of diatomic zirconium has been measured as $D_0^\circ(Zr_2)$ = 3.052 ± 0.001 eV. A discussion of the chemical bonding in the mixed early–late transition metal dimers and Zr_2 is presented, based on the measured bond energies of these species.

I. Introduction

The chemical bonding between transition metal atoms is an area of interest to many different branches of chemistry, including metallurgy, surface science, and metal cluster chemistry. Unraveling the details of the complicated electronic structure in these metallic species is an ongoing process pursued through both experimental[1,2] and theoretical[3,4] avenues. From this research it is already clear that several distinct factors combine to determine the strength and character of the chemical bond between transition metal atoms. One such factor is the loss of exchange energy which occurs upon formation of d-electron bonds, thereby reducing the strength of the chemical bonding. This is illustrated in the example of Ti_2,[5] where exchange effects favor the $4s\sigma_g^2 3d\pi_u^4 3d\sigma_g^1 3d\delta_g^1$, $^3\Delta_{g,r}$ state as a candidate for the ground state, while bonding considerations favor the $4s\sigma_g^2 3d\pi_u^4 3d\sigma_g^2$, $^1\Sigma_g^+$ state. In Ti_2 the balance between exchange effects and chemical bonding is so delicate that *ab initio* theory is incapable of determining which possibility is the ground state.[5] Experimentally it is found that exchange effects dominate in Ti_2, leading to an X $^3\Delta_{g,r}$ ground state.[6] In the isovalent Zr_2 molecule, however, the larger d-orbitals favor bond formation, leading to a strong theoretical prediction of a $^1\Sigma_g^+$ ground state.[5,7] Thus, to understand the bonding in the diatomic transition metals the competing effects of exchange and chemical bonding must be carefully considered.

Another competing factor which plagues the understanding of chemical bonding in the diatomic transition metals is that often the strongest chemical bond results from combining excited-state atoms. For transition metals with ground states of d^ns^2, the strongest chemical bonds generally result when the atoms are promoted to the excited $d^{n+1}s^1$ atomic limit. This excited configuration of the atoms is now capable of forming a strong $s\sigma^2$ bond, and in the early transition metals strong d-orbital bonding is possible as well. In systems where d ← s promotion is required to reach the $d^{n+1}s^1$ limit, however, it can be difficult to determine whether the bonding energy gained is sufficient to overcome the energetic cost of promotion to the excited $d^{n+1}s^1$ configuration.

Work in this group has concentrated on investigating the electronic structure of diatomic transition metals through spectroscopic methods.[6,8-15] In addition to the spectroscopic determination of the ground-state term symbol, electronic configuration, bond length, and vibrational frequency, another piece of information which is valuable for understanding the nature of transition metal bonding is the bond dissociation energy, which represents the sum of all the interactions occurring between the atoms. In the present investigation we report bond strength measurements of several mixed early–late transition metal diatomics, specifically the diatomic combinations of the early 4d metals yttrium, zirconium, and niobium with the late 3d metals cobalt and nickel. These metal species are of interest because of the combination of an electropositive early transition metal with an electronegative late transition metal, which creates the possibility of an ionic contribution to the bonding by donation of s electron density from the early transition metal to the late transition metal. In addition to this transfer of s-electron density to the more electronegative late transition metal, there is also the possibility of significant back-donation of d-electron density to the early transition metal atom, which is d-electron deficient. This is the essence of the Brewer–Engel model of transition metal bonding,[16] which predicts the mixed early–late transition metal molecules to be more strongly bound than their homonuclear counterparts. Measurements of the bond strengths of these molecules will help to clarify the applicability of this model to the smallest systems.

Previously, the bond dissociation energies of TiV,[8] V_2,[8] TiCo,[8] VNi,[8] Ni_2,[9] NiPt,[10] Pt_2,[11] AlNi,[12] Co_2^+,[13] Ti_2^+,[14] V_2^+,[14] and Co_3^+ [14] have been measured by the abrupt onset of predissociation in an extremely congested optical spectrum. To this list we now add seven new bond strengths measured by this method: Zr_2, YCo, YNi, ZrCo, ZrNi, NbCo, and NbNi. The factors contributing to the bonding in these species, along with periodic trends among the growing number of intermetallic metals which have been investigated, are also discussed.

II. Experimental Section

The intermetallic molecules listed above are created by pulsed laser vaporization of a metal alloy disk in the throat of a pulsed supersonic expansion of helium. The ablated metal atoms are expelled into a 2-mm channel just prior to the peak density of the helium pulse, are entrained in the helium flow, and undergo supersonic expansion into vacuum from a 2-mm orifice approximately 3 cm downstream from the point of vaporization. Although larger clusters are also produced, by carefully controlling the firing time of the vaporization laser (Nd:YAG second harmonic, 15 mJ/pulse) and the backing pressure of helium, one

* Abstract published in *Advance ACS Abstracts*, January 15, 1994.

0022-3654/94/2098-1398$04.50/0

may decrease the number of larger clusters produced to a minimum. This reduces the possibility of fragmentation of larger clusters, which can obscure the true spectroscopic processes occurring in the diatomic metals. In the present study of the intermetallic metal dimer bond strengths, a resonant two-photon ionization (R2PI) process is used to investigate the species present in the molecular beam. The specifics of the R2PI instrument are more completely described elsewhere.[17]

Based on previous studies from this group, rotational temperatures of 3–10 K and vibronic temperatures of 100–500 K are expected from this source. The presence of vibronically hot molecules in the molecular beam should not affect the interpretation of the data, because these hot molecules possess a minimum of 50–100 cm^{-1} of vibronic energy and should therefore predissociate at energies at least 50–100 cm^{-1} below that required for molecules in the ground state, which in any case constitute the majority of species in the beam. Our measured predissociation thresholds are typically defined to ±2 cm^{-1}, which is inconsistent with any broadening of the threshold which might be associated with the population of excited vibronic levels. At rotational temperatures of 3–10 K, the rotational energy of the molecules is 2–7 cm^{-1}, and on this basis an uncertainty of ±0.001 eV (±8 cm^{-1}) is assigned to the measured bond energies.

An unusual and powerful aspect of this molecular beam apparatus is the use of a metal alloy target disk instead of the more conventional metal rod source. The metal alloy source disks used in this investigation were produced in an electric arc furnace capable of reaching a temperature of 3500 °C. The sample is prepared by placing weighed amounts of the individual lump metals, approximately 10–15 g total, in the electric arc furnace. An arc (100 A, 40 V) is then struck above the metal pieces, which are enclosed in an inert atmosphere of argon. Complete melting of the metals is typically achieved when the arc current is increased to 200 A. After cooling, the alloyed metal nugget is turned over and remelted. After three or four repetitions, the convection currents in the molten metal lead to a completely homogeneous mixed metal sample. The alloy disk is then ground to provide a flat surface for laser vaporization, which greatly reduces intensity fluctuations in the molecular beam as the sample is translated and rotated to present a fresh surface for laser vaporization.

The mole ratio of the constituent metals in the alloy can exert a powerful influence on the abundance of the diatomic metals in the molecular beam. Our experimentally developed rule of thumb is that the ratio of the bond strengths of the respective dimers should be inversely related to the elemental concentrations in the alloy in order to optimize production of the intermetallic dimer. As an example, the bond strength of Ni_2 is 2.068 ± 0.010 eV,[9] roughly a factor of 3 less than the bond strength of Nb_2 (5.21 ± 0.10 eV).[18] Accordingly, a 1:3 alloy of Nb:Ni was prepared to study the NbNi molecule. By using an alloy that was enriched in the element forming the weaker bonds, the exothermic displacement reaction

$$NbNi + Nb \rightarrow Nb_2 + Ni$$

could be partially overcome, allowing a usable concentration of NbNi molecules to be produced. For the studies of the YNi, YCo, ZrNi, and ZrCo molecules, alloys were prepared in a 1:1 ratio, while a 1:3 molar ratio alloy of NbCo was prepared for investigations of this molecule.

The jet-cooled mixed metal cluster beam passes through a 1-cm skimmer, sending a collimated beam into the ionization region of a time-of-flight mass spectrometer, where a Nd:YAG pumped dye laser is used to excite the molecules by collinear propagation down the molecular beam axis. Excited molecules are then ionized by the output of an excimer laser operating on KrF (5.00 eV, 248 nm), which crosses the molecular beam at right angles and is fired about 10–20 ns after the excitation dye laser. A mass-selected optical spectrum of ion signal *vs* frequency is collected by scanning the dye laser. For most of the molecules investigated, the dye laser was calibrated using well-known transitions of atomic zirconium.[19] In the case of YNi, however, the dye laser was calibrated by narrowing the output using an intracavity etalon (0.04 cm^{-1}) and pressure scanning with Freon-12 (CCl_2F_2, DuPont). The output was Raman shifted using high-pressure (500-psi) H_2, and the Stokes-shifted radiation was used to collect an I_2 absorption spectrum for comparison to the atlas of Gerstenkorn and Luc.[20] Using the known Raman shift (4155.163 cm^{-1})[21] of the H_2 Q(1) transition at 500 psi (34 atm) allowed the fundamental radiation of the dye laser to be precisely calibrated. For all of the molecules studied, a generous absolute error estimate of ±8 cm^{-1} (±0.001 eV) is assigned to the dissociation energy, even though the dye laser was calibrated to an accuracy of better than ±2 cm^{-1}.

III. Results

In previous studies from this group we have reported abrupt predissociation thresholds in a congested optical spectrum for several open d-subshell transition metal diatomics and have argued that these thresholds correspond to the thermochemical bond strength of the molecule.[8-14] Our contention has been that in most of the open d-subshell diatomics the density of electronic states near the dissociation limit is so high that nonadiabatic effects render the concept of motion on a single Born–Oppenheimer potential energy surface untenable. Because of nonadiabatic couplings between electronic states, in most examples a sharp onset of predissociation then occurs as soon as the energy of separated ground-state atoms is exceeded. In several examples (such as Ni_2,[9] Pt_2,[11] Co_2^+,[13] Ti_2^+,[14] and V_2^+ [14]) the bond strengths derived from predissociation thresholds are in excellent agreement with values determined through other methods, lending credence to the argument. In the few cases where abrupt thresholds are observed which differ from the results of other measurements (as is the case for Cr_2^+ [22,23]), specific reasons for the disagreement are usually evident. In the case of Cr_2^+, for example, the lowest separated atom limits are $d^5s^1(^7S,^5S) + d^5(^6S)$, and the lack of orbital angular momentum leads to a low density of electronic states. Further, all of the states which arise from these limits are Σ^+ states, which cannot be coupled to one another through spin–orbit interactions.[25] In another set of examples, NiPd and PdPt failed to display a sharp predissociation threshold despite a high density of excited electronic states evident in the spectrum.[15] These species possess only attractive potential curves arising from ground-state atoms, however, and the nesting of the resulting potential curves may have prevented a sharp onset of predissociation. Even when the lowest separated atom limits generate only attractive curves, however, a sharp predissociation threshold may still be identified with the bond strength, as was found in the case of Co_2^+.[13] In the photodissociation spectrum of this molecule, a sharp predissociation threshold provides a bond strength ($D_0^0(Co_2^+)$ = 2.765 ± 0.001 eV) which is in excellent agreement with the results of a collision-induced dissociation study ($D_0^0(Co_2^+)$ = 2.75 ± 0.10 eV).[26]

These examples have been previously discussed, and criteria have been developed as a guide to when an abrupt onset of predissociation may be expected to occur and to correspond to the thermochemical bond strength.[8,13] The most important of these criteria is that the molecule must possess a large density of electronic states. To investigate the expected density of electronic states in these molecules, it is a simple matter to determine the number of case (c) potential curves arising from each separated atom limit. In combining two atoms in spin–orbit levels with total angular momentum J_A and J_B, $(2J_A + 1)(2J_B + 1)/2$ distinct relativistic adiabatic (Hund's case (c)) potential curves are obtained if $J_A + J_B$ is half-integer, while $(2J_< + 1)(J_> + 1)$ distinct curves result if $J_A + J_B$ is an integer.

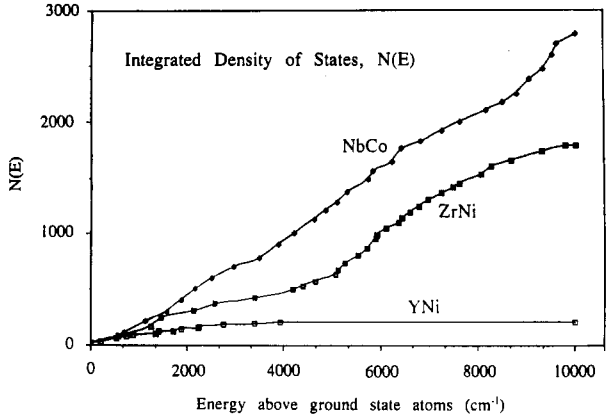

Figure 1. This figure displays the number of Hund's case (c) potential curves arising within an energy E of ground-state atoms for YNi, ZrNi, and NbCo, for energies up to 10 000 cm^{-1}. Abrupt predissociation is expected in these molecules because of the large density of electronic states, many of which may be expected to dip below the ground separated atom limit. The remarkable difference in the density of states between these molecules underscores the complexity of establishing periodic trends in transition metal compounds.

Summing the number of potential curves arising from all separated atom limits below an energy, E, then results in an integrated density of electronic states at the separated atom limit, $N(E)$. Although this function pertains to the separated atoms, it nevertheless provides a good indication of the expected state density in the diatomic molecule. The density of electronic states calculated in this way for the mixed early–late diatomic molecules is quite large for all of the species studied here. Nevertheless, the actual number of states varies significantly from molecule to molecule. For example, 205 Hund's case (c) potential curves arise within 10 000 cm^{-1} of ground separated atoms in YNi while 2780 potential curves arise within the same energy range in NbCo. Figure 1 displays the integrated density of states, $N(E)$, for the mixed early–late transition metal dimers YNi, ZrNi, and NbCo.

From the results reported below, it appears that the vastly different number of potential curves in these species makes no noticeable difference in the sharpness of the predissociation threshold. Nevertheless, the differences in state density are apparent in the optical spectra of these molecules. For example, NbNi, which generates 1828 potential curves within 10 000 cm^{-1} of ground-state atoms, shows only a continuous absorption spectrum below the dissociation limit in Figure 2b, while YNi, which generates only 205 potential curves within 10 000 cm^{-1} of the ground separated atom limit, displays discrete vibronic bands in addition to an underlying continuum in Figure 3b. These two examples show how an increase in the number of potential curves causes the vibronic structure to wash out in the spectra of diatomic transition metal molecules.

A. Zr_2. Although diatomic zirconium is the only molecule in this study not classified as an early–late species, it provides both the most interesting spectrum and the strongest evidence of predissociation at the thermodynamic threshold. The spectrom of Zr_2 was originally collected at the same time as the spectrum of ZrCo, a terrific advantage of a mass-resolved experiment. Because a 1:1 molar alloy of Zr:Co was employed, the molecular beam was only 50% zirconium in composition, and the opportunity for the production of large zirconium clusters was significantly diminished. We have previously found that photofragmentation of large clusters can create a false ion signal at the mass of the dimer, spoiling the possibility of recording a true dimer spectrum. The elimination of large clusters by use of a mixed alloy target made it possible to record a resonant two-photon ionization spectrum of Zr_2.

The ground state of Zr_2 has been theoretically determined to be $5s\sigma_g^2 4d\pi_u^4 4d\sigma_g^2$, $^1\Sigma_g^+$, yielding $\Omega = 0_g^+$ in Hund's case (c) notation.[5,7] Electric dipole allowed transitions from the ground

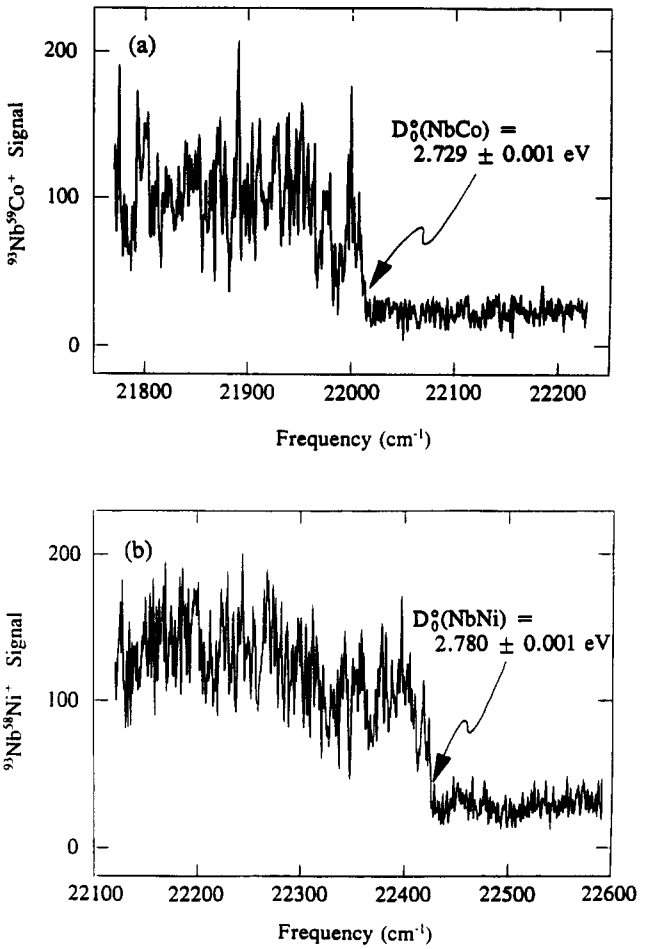

Figure 2. Resonant two-photon ionization spectra of NbCo (a) and NbNi (b) taken near their respective dissociation energies. The NbCo spectrum, collected using a dye laser operating on coumarin 460 in conjunction with KrF excimer radiation, shows a threshold at 22 014 cm^{-1}, yielding a bond strength of D_0°(NbCo) = 2.729 ± 0.001 eV. The NbNi spectrum was collected using KrF excimer radiation for ionization and coumarin 440 dye laser radiation for excitation and displays a predissociation threshold at 22 425 cm^{-1}, resulting in a bond strength of D_0°(NbNi) = 2.780 ± 0.001 eV.

state can therefore only populate $\Omega = 0_u^+$ or $\Omega = 1_u$ states. However, the combination of two ground-state zirconium atoms ($4d^25s^2$, $^3F_2$) can only lead to 4_g, 3_u, 3_g, 2_u, $2_g(2)$, $1_u(2)$, $1_g(2)$, $0_u^-(2)$, and $0_g^+(3)$ Hund's case (c) states of the dimer.[24] Notably absent from this set are the optically accessible 0_u^+ states. Therefore, the 0_u^+ states which are accessed when the ground 0_g^+ state absorbs a photon cannot predissociate to ground-state atoms while preserving their good quantum numbers, Ω, g/u, and $0^+/0^-$. The 0_u^+ states that are accessed should therefore persist in the optical spectrum until a separated atom limit generating 0_u^+ states is reached. This unusual situation is apparent in Figure 4, where two predissociation thresholds are evident, at 24613 ± 2 and 25183 ± 2 cm^{-1}, respectively. It is interesting that the predissociation thresholds are quite evident in the spectrum displayed in Figure 4, despite the fact that this was a one-color experiment. By this we mean that the states probed in Figure 4 lie at an energy which is more than halfway to the ionization limit, so the same wavelength used to excite the molecule could also be used to ionize it. Despite the fact that there was no time delay between the excitation and ionization laser pulses (since they were in fact the same pulse), the intially excited state nevertheless predissociates so rapidly that it cannot be ionized by the absorption of a second photon. This proves that the predissociation occurs on a time scale faster than 5 ns.

The separation between the two predissociation thresholds (570 ± 3 cm^{-1}) matches the spin–orbit excitation energy of the

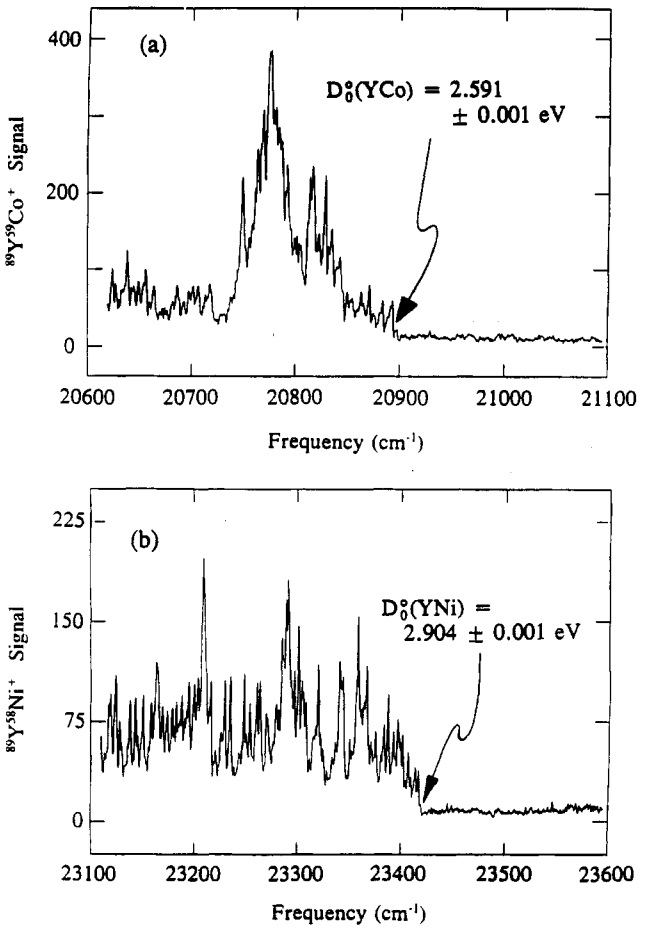

Figure 3. Predissociation thresholds in YCo (a) and YNi (b) observed by resonant two-photon ionization using dye laser radiation from coumarin 480 and stilbene 420 dyes, respectively, and KrF excimer radiation for ionization. The predissociation threshold in YCo occurs at 20 898 cm^{-1}, yielding a bond strength of D_0°(YCo) = 2.591 ± 0.001 eV. In YNi the predissociation threshold occurs at 23 420 cm^{-1}, providing a bond energy of D_0°(YNi) = 2.904 ± 0.001 eV.

zirconium atom (571.41 cm^{-1})[19] within experimental error, showing that the second threshold corresponds to dissociation to the Zr($4d^25s^2$, $^3F_2$) + Zr($4d^25s^2$, $^3F_3$) spin–orbit excited limit. This separated atom limit does indeed generate 0_u^+ potential curves,[24] substantiating the idea that predissociation does not occur until a limit generating the appropriate values of the good quantum numbers Ω, g/u, and $0^+/0^-$ is reached.

This situation in Zr_2 is very similar to previous observations in V_2,[8] where the $^3\Sigma_g^-(0_g^+)$ ground state creates an identical mechanism for a double predissociation threshold. In the case of V_2, the separation between the two predissociation thresholds is also in agreement with the energy separation between the ground and first excited state separated atom limits. Together, these double threshold examples suggest strongly that the abrupt predissociation threshold corresponds to the true bond strength. This allows us to confidently expect that the abrupt predissociation thresholds measured for other open d-subshell species will also give accurate bond strengths. We also note that if all of the 0_u^+ states excited were immune to predissociation prior to the first excited atomic limit, the ratio of the signal intensities above and below the first threshold should reflect the numbers of 0_u^+ and 1_u states in this energy region. If this were the case, a drop in signal of about two-thirds would be expected at the first threshold, in stark contrast to the larger drop that is observed. It is obvious that a (rotationally induced) heterogeneous coupling mechanism allows 0_u^+ states to mix with dissociative 1_u states in this energy region. Another indication of this phenomenon was our initial failure to detect a second threshold under expansion conditions which populated higher energy rotational states of Zr_2. Only after more extensive rotational cooling was achieved by using a smaller expansion orifice were the dissociation rates of the 0_u^+ states reduced sufficiently for the second threshold to be observed. This is in agreement with a heterogeneous coupling mechanism, where the coupling matrix elements are proportional to $\sqrt{J(J+1)}$.[25]

Converting the predissociation threshold at 24613 ± 2 cm^{-1}, one obtains a bond strength of $D_0^\circ(Zr_2)$ = 3.052 ± 0.001 eV. To our knowledge, this is the first experimental measurement of this quantity. Several theoretical calculations and semiempirical estimates have been made, however. The estimate of $D_0^\circ(Zr_2)$ = 3.22 ± 0.2 eV by Miedema and Gingerich[27] using an extrapolation from bulk metal properties proves to be the most accurate. *Ab initio* quantum chemical treatments of the bonding in Zr_2 have underestimated the bond strength, with Balasubramanian and Ravimohan reporting a value of $D_0^\circ(Zr_2)$ = 2.45 eV calculated at the state-averaged complete active space self-consistent field/multireference singles + doubles configuration interaction (SA-CASSCF-MRSDCI) level[7] and Bauschlicher *et al.* reporting a value of $D_0^\circ(Zr_2)$ = 2.21 eV using an averaged coupled-pair functional treatment.[5] Underestimation of dissociation energies is a common difficulty in calculations of systems which require an accurate description of d–d bonding, primarily because electron correlation is more accurately described in the separated atoms than in the molecule. Improvements in the calculation by Balasubramanian and Ravimohan including higher-order correlations and extended basis sets have resulted in a final bond strength prediction of 2.7 eV ≤ $D_0^\circ(Zr_2)$ ≤ 3.0 eV.[7] This revised value lies just at the limit of our experimental measurement, $D_0^\circ(Zr_2)$ = 3.052 ± 0.001 eV.

B. YNi and YCo. The ground state of YNi is known to be X $^2\Sigma$ by matrix isolation ESR spectroscopy.[28] From the Ω = 1/2 ground state, Ω = 1/2 and Ω = 3/2 excited states are optically accessible under electric dipole selection rules. The lowest separated atom limit for YNi, corresponding to Y($4d^15s^2$, $^2D_{3/2}$) + Ni($3d^84s^2$, $^3F_4$), generates Ω = 1/2 and Ω = 3/2 states (along with many others), so the excited states reached upon optical excitation can fall apart to ground-state atoms while preserving the good quantum number, Ω. Spectroscopically, this is shown in Figure 3b, where a sharp predissociation threshold is observed at 23420 ± 2 cm^{-1}. Converting to electronvolts and using a more generous error limit then provide D_0°(YNi) = 2.904 ± 0.001 eV. This mixed metal bond strength is much greater than that of either of the homonuclear dimers, Y_2 (1.62 ± 0.22 eV)[29] or Ni_2 (2.068 ± 0.010 eV),[9] in agreement with the Brewer–Engel model.[16]

A comprehensive theoretical investigation of the YNi molecule has been performed by Faegri and Bauschlicher.[30] Their study suggests that the X $^2\Sigma^+$ ground state is best correlated to a Y($4d^15s^2$) + Ni($3d^94s^1$) asymptote, a possibility discussed in section IV below. As was mentioned in connection with Zr_2 above, such theoretical calculations usually underestimate molecular bond strengths because the correlation energy of the separated atoms is more accurately calculated than that of the molecule. This is also the case in YNi, where the best bond strength estimate is obtained at the CASSCF-MRCI level including relativistic corrections as D_0°(YNi) = 2.01 eV.[30] This severe underestimate of the YNi bond strength highlights the difficulty in estimating bond strengths of diatomic transition metals by *ab initio* methods.

An abrupt predissociation threshold is also found in the resonant two-photon ionization spectrum of YCo at 20898 ± 2 cm^{-1}, as displayed in Figure 3a. This converts to a bond strength of D_0°(YCo) = 2.591 ± 0.001 eV. Again this mixed metal diatomic has a much greater bond strength than either of its homonuclear counterparts, with $D_0^\circ(Y_2)$ = 1.62 ± 0.22 eV[29] and $D_0^\circ(Co_2)$ = 0.95 ± 0.26 eV.[31] In addition, the resonant two-photon ionization spectrum of YCo shows strong intensity right at the threshold,

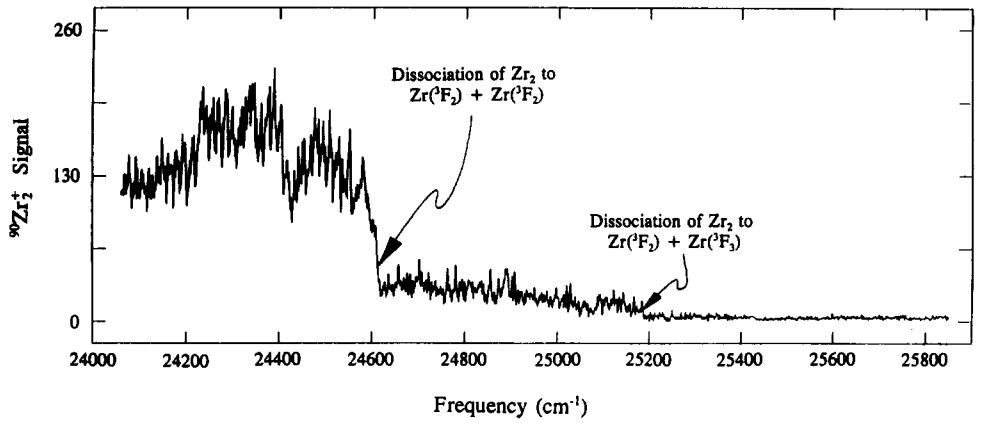

Figure 4. Resonant two-photon ionization spectrum of Zr_2 near its dissociation limit. The spectrum is a composite of scans collected using exalite 398 and exalite 404 dye laser radiation, both to excite and to ionize Zr_2 in a one-color resonant two-photon ionization scheme. A predissociation threshold at 24 613 cm^{-1} gives the bond energy of Zr_2, $D_0^\circ(Zr_2) = 3.052 \pm 0.001$ eV. Above this energy, however, a weaker absorption continnum persists to 25 183 cm^{-1}, which corresponds to a second predissociation threshold. The second predissociation threshold in Zr_2 is a result of rotationally cold 0_u^+ states which are excited by transitions from the ground X $\Omega'' = 0_g^+$ level and which cannot predissociate to the lowest atomic limit.

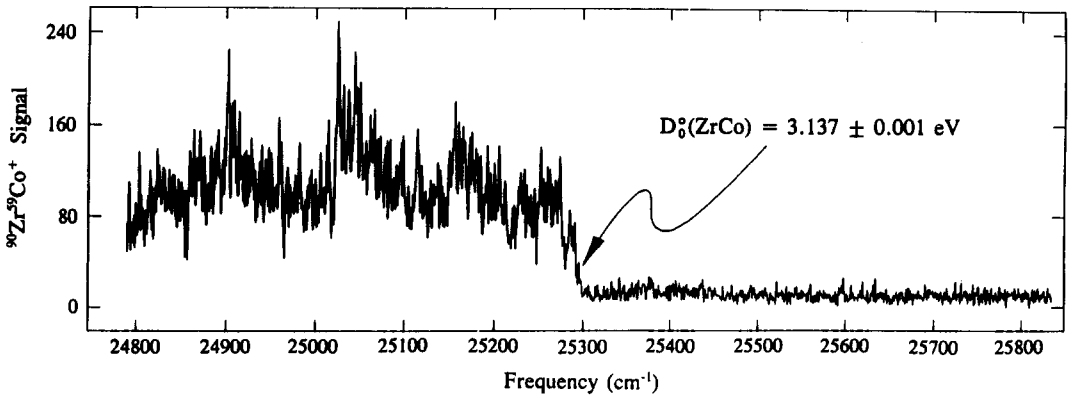

Figure 5. Predissociation threshold of ZrCo, observed by resonant two-photon ionization spectroscopy using exalite 398 and exalite 389 dye laser radiation in conjunction with KrF excimer laser radiation for photoionization. The observed predissociation threshold at 25 298 cm^{-1} corresponds to a bond strength of $D_0^\circ(ZrCo) = 3.137 \pm 0.001$ eV.

which decreases to a more moderate signal at lower frequencies. The reason for such behavior is not at all understood; similar spectral rises as one approaches the dissociation threshold are also observed in TiCo[8] and VNi,[8] however.

C. ZrCo and ZrNi. The predissociation threshold of ZrCo at 25298 ± 2 cm^{-1}, displayed in Figure 5, results in the largest bond strength measured in this study, $D_0^\circ(ZrCo) = 3.137 \pm 0.001$ eV. The large bond strength of ZrCo may indicate that of the six mixed early–late transition metal diatomics studied ZrCo is the candidate best suited for application of the Brewer–Engel bonding model.[16] In this model the d-electron density of cobalt overlaps significantly with the zirconium d-orbitals, leading to strong multiple d-bonds.

Although ZrNi is not bound as strongly as ZrCo, it nevertheless possess a significant bond strength of $D_0^\circ(ZrNi) = 2.861 \pm 0.001$ eV, as measured from the abrupt predissociation threshold shown in Figure 6 at 23072 ± 2 cm^{-1}. A reverse correlation between bond strength and promotion energy is observed in ZrCo and ZrNi. Although cobalt must expend 0.482 eV more in promotion energy than nickel,[19] the measured bond strength of ZrCo is nevertheless greater than that of ZrNi. This indicates a significant d-orbital bonding contribution in these molecules; otherwise, one would expect the difference in bond strengths to correlate directly with the difference in promotion energies.

D. NbNi and NbCo. Diatomic NbNi and NbCo show sharp predissociation thresholds in their resonant two-photon ionization spectra at 22425 ± 2 and 22014 ± 2 cm^{-1}, respectively, as shown in Figure 2. These correspond to bond strengths of $D_0^\circ(NbNi) = 2.780 \pm 0.001$ eV and $D_0^\circ(NbCo) = 2.729 \pm 0.001$ eV. The close similarity in bond strength between these two compounds

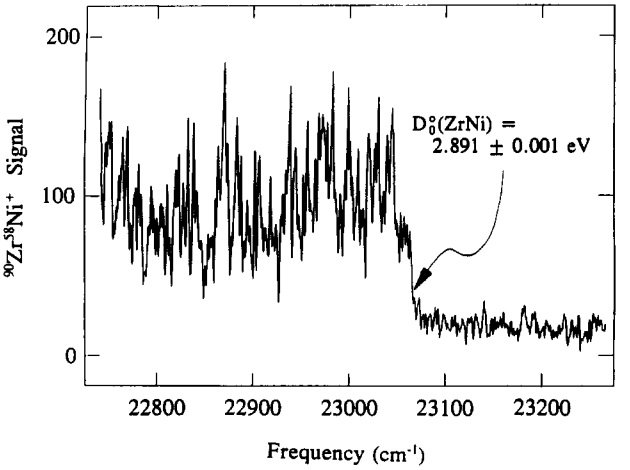

Figure 6. Resonant two-photon ionization spectrum of ZrNi, exhibiting a predissociation threshold at 23 072 cm^{-1}. The spectrum was recorded using coumarin 440 dye laser radiation for excitation along with KrF excimer radiation for ionization. The measured predissociation threshold corresponds to a bond strength of $D_0^\circ(ZrNi) = 2.891 \pm 0.001$ eV.

does not reflect the 0.482-eV difference in promotion energy between nickel and cobalt,[19] once again indicating the presence of other factors which contribute to the bonding.

IV. Discussion

The experimental measurement of the bond strengths of seven open d-subshell diatomic transition metals (Zr_2, YCo, YNi, ZrCo, ZrNi, NbCo, and NbNi) adds considerably to the increasing

TABLE 1: Bond Strengths of Selected Transition Metal Diatomics

molecule (AB)	no. of d+s electrons	D_0° (eV)	$D_0^\circ + P(B)^a$ (eV)	$D_0^\circ + P(A) + P(B)^a$ (eV)	D_0° (coinage analog) (eV)	$\langle r\rangle_{nd}$ (Å)^b atom A	atom B	ground configuration and term	ref
Ti_2	8	1.23 ± 0.17[c]	2.34 ± 0.17	3.46 ± 0.17	2.03 ± 0.02 (Cu_2)[d]	0.793	0.793	$4s\sigma_g^2 3d\pi_u^4 3d\sigma_g^1 3d\delta_g^1$, $^3\Delta_r$	6
TiCo	13	2.401[e]	3.049	4.162	2.03 ± 0.02 (Cu_2)[d]	0.793	0.544	$4s\sigma^2 3d\pi^4 3d\sigma^2 3d\delta^4 4s\sigma^{*1}$, $^2\Sigma^+$	36
VNi	15	2.100[e]	2.266	2.902	2.03 ± 0.02 (Cu_2)[d]	0.720	0.514	$4s\sigma^2 3d\pi^4 3d\sigma^2 3d\delta^4 3d\delta^{*2} 4s\sigma^{*1}$, $^4\Sigma^-$	38
Zr_2	8	3.052[f]	4.048	5.044	1.64 ± 0.04 (Ag_2)[g]	1.156	1.156	$5s\sigma_g^2 4d\pi_u^4 4d\sigma_g^2$, $^1\Sigma_g^+$	5, 7
YCo	12	2.591[f]	3.239	4.688	1.74 ± 0.10 (CuAg)[h]	1.329	0.544	$s\sigma^2 d\pi^4 d\sigma^2 d\delta^3 s\sigma^{*1}$, $^3\Delta_i$	*i*
YNi	13	2.904[f]	3.070	4.519	1.74 ± 0.10 (CuAg)[h]	1.329	0.514	$s\sigma^2 d\pi^4 d\sigma^2 d\delta^4 s\sigma^{*1}$, $^2\Sigma^+$	28
ZrCo	13	3.137[f]	3.785	4.781	1.74 ± 0.10 (CuAg)[h]	1.156	0.544	$s\sigma^2 d\pi^4 d\sigma^2 d\delta^4 s\sigma^{*1}$, $^2\Sigma^+$	*i*
ZrNi	14	2.861[f]	3.027	4.023	1.74 ± 0.10 (CuAg)[h]	1.156	0.514	$s\sigma^2 d\pi^4 d\sigma^2 d\delta^4 d\delta^{*1} s\sigma^{*1}$, $^3\Delta_r$	*i*
NbCo	14	2.729[f]	3.377	3.901	1.74 ± 0.10 (CuAg)[h]	1.127	0.544	$s\sigma^2 d\pi^4 d\sigma^2 d\delta^4 d\delta^{*1} s\sigma^{*1}$, $^3\Delta_r$	*i*
NbNi	15	2.780[f]	2.946	3.470	1.74 ± 0.10 (CuAg)[h]	1.127	0.514	$s\sigma^2 d\pi^4 d\sigma^2 d\delta^4 d\delta^{*2} s\sigma^{*1}$, $^4\Sigma^-$	38

[a] Intrinsic bond energies are defined in the text as the measured bond strength plus the promotion energy required to prepare the atoms for bonding, where the promotion energy of atom B, $P(B)$, is defined by performing a weighted average of the spin–orbit levels of the high- and low-spin couplings of the s^1 electron to the lowest term of the d^n core. This gives the energies of these terms in the absence of spin–orbit coupling. These are then averaged to obtain the energy of the hypothetical spin-decoupled s^1–d^n state above the ground state, which is defined as $P(B)$. In the column headed $D_0^\circ + P(B)$, only the late transition metal atom is assumed to promote, while in the column headed $D_0^\circ + P(A) + P(B)$ it is assumed that both atoms are promoted. Atomic energy levels are taken from ref 19. [b] From ref 33. [c] From ref 2. [d] From ref 39. [e] From ref 8. [f] This work. [g] From ref 40. [h] From ref 35. [i] Suggested to be the ground state in the present investigation.

pool of information available about the chemical bonding in these complex transition metal systems. A summary of the measured bond strengths and other pertinent information about these species is provided in Table 1.

A problem in understanding the chemical bonding in the transition metal diatomic molecules is the question of which separated atom limit leads to the ground state of the molecule. As mentioned in section I, the strongest chemical bonds generally result from the interaction of a $d^{n+1}s^1$ atom with a $d^{m+1}s^1$ atom, which leads to a strong s-based σ^2 bond. Although this can also arise from the interaction of a $d^n s^2$ atom with a $d^{m+2}s^0$ atom, this separated asymptote nearly always lies considerably higher in energy than the $d^{n+1}s^1 + d^{m+1}s^1$ limit in the neutral transition metal diatomics. Thus, in most cases the ground state of the separated atoms cannot correlate to the strongly bound $s\sigma^2 d^{n+1}d^{m+1}$ molecular configuration, and an amount of energy must be expended to excite the atoms to an appropriate separated atom limit in preparation for bonding. As a consequence, the ground state of the molecule often may depend on a delicate balance between the energy gain due to chemical bonding and the energetic cost of preparing the atoms for bonding (i.e., their promotion energy).

In computing the promotion energy, it is useful to remember that when one forms an $s\sigma^2$ chemical bond between a $d^{n+1}s^1$ atom and a $d^{m+1}s^1$ atom, one does not gain the full strength of the $s\sigma^2$ bond because of the loss of the d^{n+1}–s^1 and d^{m+1}–s^1 exchange energy in the high spin coupled $d^{n+1}s^1$ and $d^{m+1}s^1$ atomic states. Thus, one should consider the promotion energy to be the amount of energy required to excite the atom to a hypothetical state lying halfway between the high- and low-spin couplings of the s^1 electron to the d^{n+1} or d^{m+1} core. This approach has been used to calculate the promotion energies for transition metal atomic cations bonding to a hydrogen atom, and a clear correlation of bond strength with promotion energy has been found.[32] We note that this represents a refinement in the definition of promotion energy as compared to our previous use of the term.[8]

Using the promotion energy defined in this way, we have also calculated intrinsic bond energies for the molecules reported in this investigation. These intrinsic bond strengths are defined as the bond strengths that would be expected if an $s\sigma^2 d_A^n d_B^{m+1} s\sigma^{*1}$ AB molecule dissociated diabatically to the $d^n s^2$ (atom A) + the hypothetical spin-decoupled $d^{m+1}s^1$ (atom B) separated atom asymptote. Intrinsic bond strengths defined in this way are listed in column four of Table 1 as $D_0^\circ + P(B)$. Alternatively, the ground state may be $s\sigma^2 d_A^{n+1} d_B^{m+1}$, which diabatically correlates to the doubly promoted separated atom limit of $d^{n+1}s^1$ (atom A) + $d^{m+1}s^1$ (atom B), in which case both atoms must be promoted to form the ground state of the molecule. If this is the case, the intrinsic bond strength is given by $D_0^\circ + P(A) + P(B)$, listed in column five of Table 1, where $P(A)$ and $P(B)$ represent the promotion energies required to prepare the atoms in the spin-decoupled $d^{n+1}s^1$ and $d^{m+1}s^1$ states, respectively. In all cases listed in Table 1, the early transition metal atom (Ti, V, Y, Zr, or Nb) is designated as atom A and the late transition metal atom (Co or Ni) is designated as atom B. With the single exception of NbCo, the third alternative of diabatic correlation of an $s\sigma^2 d_A^{n+1} d_B^m s\sigma^{*1}$ state to the spin-decoupled $d^{n+1}s^1$ (atom A) + $d^m s^2$ (atom B) separated atom limit need not be considered, since this limit lies above the $d^n s^2$ (atom A) + $d^{m+1}s^1$ (atom B) asymptote, and therefore the lower asymptote will generate the favorable $s\sigma^2 s\sigma^{*1}$ conditions for bonding.

From the preceding commentary, it is clear that the separated atom parentage of the ground state of the diatomic molecule will be an important consideration. Unfortunately, in only a few of the examples considered here is there any evidence, either experimental or theoretical, that speaks to this point. This question will be addressed further in the discussions of the individual molecules below.

A. Zr_2. As mentioned above, the homonuclear diatomic molecule, Ti_2, is now experimentally known to possess a $4s\sigma_g^2 3d\pi_u^4 3d\sigma_g^1 3d\delta_g^1$, $^3\Delta_{g,r}$ ground state,[6] where $4s\sigma$–$3d\sigma$ hybridization is thought to stabilize the "$4s\sigma_g$" orbital and destabilize the "$3d\sigma_g$" orbital, resulting in an unexpected orbital filling order. This ground state correlates to the doubly promoted $3d^3 4s^1$, ^5F + $3d^3 4s^1$, ^5F separated atom limit, which greatly decreases the measured bond strength of the molecule due to the high promotion energy associated with preparation of the spin-decoupled $3d^3(^4F)$–$4s^1$ state of the titanium atom (1.113 eV per atom) and the relatively poor 3d bonding that results because of the small size of the 3d orbitals.

In the isovalent Zr_2 molecule, on the other hand, the orbital radii of the 4d and 5s orbitals are more similar ($\langle r_{4d}\rangle/\langle r_{5s}\rangle$ = 0.549 in Zr $4d^2 5s^2$, ^3F)[33] than are the radii of the analogous 3d and 4s orbitals in titanium ($\langle r_{3d}\rangle/\langle r_{4s}\rangle$ = 0.401 in Ti $3d^2 4s^2$, ^3F),[33] making d-orbital bonding more favorable in diatomic zirconium than in diatomic titanium. In addition, the promotion energy required to prepare a zirconium atom in a spin-decoupled $4d^3(^4F)$-$5s^1$ state is reduced slightly from that of titanium, to 0.996 eV per atom. On these grounds we may confidently expect that the ground state of Zr_2 derives from two spin-decoupled $4d^3(^4F)$–$5s^1$ atoms. Indeed, *ab initio* calculations are now in general agreement that the ground state of Zr_2 is $5s\sigma_g^2 4d\pi_u^4 4d\sigma_g^2$, $^1\Sigma_g^+$.[5,7] This conclusion is also in agreement with the observation of a double predissociation threshold, as discussed

above. Thus, the intrinsic bond strength of Zr_2 is 5.044 eV, in comparison to an intrinsic bond strength of only 3.46 ± 0.17 eV for Ti_2 (based on the value $D_0^\circ(Ti_2)$ = 1.23 ± 0.17 eV).[2] Undoubtedly the enhanced intrinsic bond strength of Zr_2 as compared to Ti_2 results from the improved overlap between the d orbitals in zirconium as compared to titanium. This improved d-electron bonding also favors spin-pairing of the 4d electrons in the $4d\sigma_g$ orbital, leading to the $^1\Sigma_g^+$ state calculated to be the ground state of Zr_2.[5,7] In the remaining molecules investigated in the present study, the compact nature of the 3d orbitals will continue to play an important role in limiting the extent of d orbital contributions to the bonding, particularly as one moves to the right in the 3d transition metal series.

B. YNi and YCo. Van Zee and Weltner have determined the ground electronic state of matrix-isolated YNi to be $^2\Sigma$ by electron spin resonance (ESR) spectroscopy.[28] Their analysis of the hyperfine coupling associated with the $I = 1/2$ ^{89}Y nucleus in YNi shows the unpaired σ electron to have 30% $5s_Y$ character and 80% $4d_Y$ character, a result that does not conserve probability. This apparently erroneous result occurs because the analysis cannot determine the amounts of $4d_Y$, $5s_Y$, and $5p_Y$ character independently, since only two independent parameters (the isotropic and dipolar components of the ^{89}Y hyperfine coupling tensor) are measured. The $5p_Y$ hyperfine interaction is larger than the $4d_Y$ hyperfine interaction, so it is likely that the unpaired σ electron occupies an orbital with substantial $5p_Y$ character, contributing strongly to the dipolar component of the hyperfine interaction tensor. Thus the experimental measurements support an electronic structure of $s\sigma^2d\pi^4d\sigma^2d\delta^4s\sigma^{*1}$, $^2\Sigma^+$, where considerable mixing of the atomic orbitals occurs within the σ framework, making the identification of orbitals as "sσ" or "dσ" tenuous at best. Indeed, throughout the entire series of early–late transition metal diatomics investigated here, it is likely that significant sσ–dσ hybridization occurs, resulting from the close proximity of the $d^{n+1}s^1$ and d^ns^2 atomic states. As a result, the nominal dσ bonding orbital is destabilized (and the nominal sσ bonding orbital is stabilized), leading to an unusual orbital filling order placing the dσ above the dπ bonding orbital (as is observed in Ti_2[5,6] and TiV,[8,34] which have ground states of $4s\sigma_g^23d\pi_u^43d\sigma_g^13d\delta_g^1$, $^3\Delta_{g,r}$, and $4s\sigma^23d\pi^43d\sigma^13d\delta^2$, $^4\Sigma^-$, respectively). Likewise, the nominal sσ^* orbital is stabilized (and the nominal dσ^* orbital is destabilized), probably making configurations of $s\sigma^2d\pi^4d\sigma^2d\delta^nd\delta^{*m}s\sigma^{*1}$ the rule rather than the exception in the molecules investigated here.

This basic concept of the electronic structure of the ground state of YNi also finds confirmation in an *ab initio* investigation by Faegri and Bauschlicher.[30] Using a complete active space self-consistent field (CASSCF) method to determine the geometry of the $^2\Sigma^+$ ground state, these investigators then used a multireference configuration interaction (MRCI) method to more accurately treat the electron correlation problem. Using the natural orbitals of the MRCI treatment, valence orbital populations of 1.84, 1.15, 0.96, and 8.96 were found for the $(5s + 5p)_Y$, $(4s + 4p)_{Ni}$, $4d_Y$, and $3d_{Ni}$ orbitals, respectively. Considering the admixture of $5p_Y$ and $4p_{Ni}$ as providing a means for the more diffuse $5s_Y$ and $4s_{Ni}$ orbitals to polarize, it makes sense to consider the ground state of the YNi molecule as deriving primarily from an $s\sigma^2d\pi^4d\sigma^2d\delta^4s\sigma^{*1}$ molecular configuration. Clearly, the excessive energetic cost of promoting the yttrium atom to the $4d^25s^1$ configuration (1.449 eV) is prohibitive in the case of its interaction with nickel. On the basis of this ground molecular configuration, the intrinsic bond strength, which would be obtained as the actual bond energy if the ground separated atom limit consisted of Y ($4d^15s^2$, ^2D) + Ni (spin-decoupled $3d^9(^2D)$–$4s^1$), is obtained from column four of Table 1 as 3.070 eV. Both this and the measured bond energy of 2.904 eV are considerably greater than the bond energy of the coinage metal analogue, CuAg (D_0°(CuAg) = 1.74 ± 0.10 eV),[35] despite the presence of an antibonding electron in the sσ^* orbital. This suggests that d-orbital contributions; ionic effects due to the combination of an early, electropositive transition metal with a late, electronegative transition metal; or both combine to substantially increase the bond strength of YNi beyond what would be expected from the sσ framework alone.

Given the excessive promotion energy required to prepare yttrium in its $5s^14d^2$ configuration, it is likely that the ground state of YCo corresponds to the removal of a weakly bonding dδ electron from YNi, giving a ground electronic state of $s\sigma^2d\pi^4d\sigma^2d\delta^3s\sigma^{*1}$, $^3\Delta_i$ for YCo. Thus, although the bond strength of YCo (2.591 eV) is considerably reduced from that of YNi (2.904 eV), the intrinsic bond strengths, calculated assuming promotion of the cobalt and nickel atoms to the spin-decoupled $3d^8(^3F)$–$4s^1$ and $3d^9(^2D)$–$4s^1$ states, respectively, are more nearly equal, taking values of 3.239 and 3.070 eV for YCo and YNi, respectively. The remaining difference in bond strengths runs counter to what one might expect, given that one additional (weakly) bonding dδ electron is present in the YNi molecule than in YCo. However, when one remembers that the 3d orbitals of nickel are more highly contracted than those of cobalt, and are hence less accessible for chemical bonding, the measured bond strengths become more understandable. In addition, if the ground state of YCo is indeed $s\sigma^2d\pi^4d\sigma^2d\delta^3s\sigma^{*1}$, $^3\Delta_i$, then an exchange stabilization between the sσ^* electron and the dδ hole will contribute to a further stabilization of the YCo bond.

C. ZrCo and ZrNi. The intermetallic dimer, ZrCo, which is isoelectronic with YNi, has the largest bond strength measured in the present study, with D_0°(ZrCo) = 3.137 ± 0.001 eV. The chemical bonding is likely to be quite similar in YNi and ZrCo, since the isovalent ScNi and TiCo molecules have been shown through matrix isolation ESR methods to bond with similar ground-state configurations of $4s\sigma^23d\pi^43d\sigma^23d\delta^44s\sigma^{*1}$, $^2\Sigma^+$.[36] Accordingly, we expect an $s\sigma^2d\pi^4d\sigma^2d\delta^4s\sigma^{*1}$, $^2\Sigma^+$ ground state for ZrCo, in analogy to that found for other 13-valence-electron early–late transition metal dimers such as YNi,[28] YPd,[28] ScNi,[28,36] ScPd,[28] and TiCo.[36]

Despite the similar ground-state configurations expected for YNi and ZrCo, the bond strength of ZrCo (D_0°(ZrCo) = 3.137 ± 0.001 eV) is significantly greater than that obtained for YNi (D_0°(YNi) = 2.904 ± 0.001 eV). Moreover, this difference in bond strength is accentuated when the intrinsic bond strength is calculated by adding the promotion energy of cobalt and nickel to the values of D_0°(ZrCo) and D_0°(YNi), giving 3.785 ± 0.001 eV and 3.070 ± 0.001 eV for ZrCo and YNi, respectively. This may be explained by the differential contraction of the 3d *vs* 4s orbitals in the 3d transition metal series as one traverses the series from left to right. This differential contraction causes the 3d orbitals to become chemically rather inaccessible in nickel, a result which is the basis for a recent success in describing the electronic structure of NiCu and Ni_2 by a ligand field method.[37] Thus, the d-orbital contributions to the chemical bonding are probably significantly reduced in YNi as compared to ZrCo, accounting for the weaker bond in the former molecule. A similar effect has been previously noted in comparing the bond strengths of TiCo (D_0°(TiCo) = 2.401 eV) and VNi (D_0°(VNi) = 2.100 eV).[8] Although the electronic configuration of VNi ($4s\sigma^23d\pi^43d\sigma^23d\delta^43d\delta^{*2}4s\sigma^{*1}$, $^4\Sigma^-$) differs from that of TiCo ($4s\sigma^23d\pi^43d\sigma^23d\delta^44s\sigma^{*1}$, $^2\Sigma^+$) by the addition of two nominally antibonding δ^* electrons, this is insufficient to explain the tremendous difference in intrinsic bond strengths of TiCo (3.049 eV) as compared to VNi (2.266 eV). Again, the highly contracted nature of the 3d orbitals in nickel greatly reduces their ability to participate in d orbital bonding. This trend is also evident in the molecules investigated in the present study, where the intrinsic bond strengths for the nickel compounds YNi, ZrNi, and NbNi are all significantly less than those of YCo, ZrCo, and NbCo (see Table 1), regardless of whether one assumes that all of these

molecules derive from promotion of just the late transition metal atom or from promotion of both atoms.

The intermetallic dimer, ZrNi, with $D_0^\circ(\mathrm{ZrNi}) = 2.861 \pm 0.001$ eV, is a 14-valence-electron system, with one more electron than either YNi or ZrCo. Assuming that the high promotion energy of zirconium (0.996 eV) forces the molecule to adopt an $s\sigma^2 s\sigma^{*1}$ configuration, the most plausible candidate for the ground state is $s\sigma^2 d\pi^4 d\sigma^2 d\delta^4 d\delta^{*1} s\sigma^{*1}$, $^3\Delta_r$, deriving from the Zr ($4d^2 5s^2$, ^3F) + Ni ($3d^9 4s^1$, ^3D) separated atom limit. Alternatively, if the zirconium atom can be promoted, the $s\sigma^2 d\pi^4 d\sigma^2 d\delta^4 d\delta^{*2}$, $^3\Sigma^-$ state deriving from the Zr ($4d^3 5s^1$, ^5F) + Ni ($3d^9 4s^1$, ^3D) separated atom limit would be the most likely candidate for the ground state. Given the very similar bond strengths of YNi (D_0°(YNi) = 2.904 eV) and ZrNi ($D_0^\circ(\mathrm{ZrNi}) = 2.861$ eV) and the large (and different) promotion energies of yttrium (1.449 eV) and zirconium (0.996 eV), it seems likely that in neither molecule is the early transition metal atom promoted. This argues in favor of an $s\sigma^2 d\pi^4 d\sigma^2 d\delta^4 d\delta^{*1} s\sigma^{*1}$, $^3\Delta_r$ ground electronic state for ZrNi. The slight decrease in bond strength in going from YNi to ZrNi then corresponds to the addition of a weakly antibonding $d\delta^*$ electron in the latter molecule.

D. NbNi and NbCo. Niobium differs from yttrium and zirconium in having a $4d^4 5s^1$, ^6D ground electronic state. Although this would lead one to expect that there would be no promotion required to prepare the niobium atom for bonding, the hypothetical spin-decoupled $4d^4(^5D)$–$5s^1$ state nevertheless lies 0.524 eV above ground-state atoms. Thus the promotion energy associated with Y, Zr, and Nb falls as one moves across the series, giving 1.449, 0.996, and 0.524 eV, respectively. The smaller promotion energy required to prepare niobium in the spin-decoupled $4d^4(^5D)$–$5s^1$ state opens up the possibility of $s\sigma^2$ ground states for NbNi and NbCo. This possibility was dismissed in the cases of YCo, YNi, ZrCo, and ZrNi but is much more plausible in the case of the niobium compounds.

Both NbCo ($D_0^\circ(\mathrm{NbCo}) = 2.729$ eV) and NbNi (D_0°(NbNi) = 2.780 eV) have bond strengths which are somewhat reduced from their neighbors, ZrCo ($D_0^\circ(\mathrm{ZrCo}) = 3.137$ eV) and ZrNi ($D_0^\circ(\mathrm{ZrNi}) = 2.861$ eV). This would be consistent with the addition of a weakly antibonding $d\delta^*$ electron to the postulated ground electronic states of ZrCo and ZrNi, suggesting ground states of $s\sigma^2 d\pi^4 d\sigma^2 d\delta^4 d\delta^{*1} s\sigma^{*1}$, $^3\Delta_r$ and $s\sigma^2 d\pi^4 d\sigma^2 d\delta^{*2} s\sigma^{*1}$, $^4\Sigma^-$ for NbCo and NbNi, respectively. Although one might think an $s\sigma^2 d\pi^4 d\sigma^2 d\delta^4 d\delta^{*2}$, $^3\Sigma^-$ and an $s\sigma^2 d\pi^4 d\sigma^2 d\delta^4 d\delta^{*3}$, $^2\Delta_i$ ground state would be conceivable for NbCo and NbNi, respectively, the ESR spectrum of NbNi conclusively demonstrates that the molecule exists as a $^4\Sigma$ molecule when isolated in a neon matrix at 4 K.[38] Unfortunately, no hyperfine splitting due to the magnetic ^{61}Ni ($I = 3/2$) nucleus was observed, so no information concerning the unpaired spin density on the nickel atom could be derived. However, a large hyperfine splitting due to the niobium ^{93}Nb ($I = 9/2$) nucleus was observed, and the isotropic component of the A tensor was used to derive that the σ orbital in the $\delta^2\sigma^1$, $^4\Sigma^-$ ground state is 28% $5s_{Nb}$ in character. Presumably a large portion of the remaining character of this σ orbital is associated with the $4s_{Ni}$ orbital, with the remainder associated with the $5p_{Nb}$, $4d\sigma_{Nb}$, $4p_{Ni}$, and possibly the $3d\sigma_{Ni}$ orbitals. The observation of an $s\sigma^2 d\pi^4 d\sigma^2 d\delta^4 d\delta^{*2} s\sigma^{*1}$, $^4\Sigma^-$ ground state for NbNi argues strongly for an $s\sigma^2 d\pi^4 d\sigma^2 d\delta^4 d\delta^{*1} s\sigma^{*1}$, $^3\Delta_r$ ground state in NbCo. Accordingly, we compute their intrinsic bond strengths as D_0°(NbNi) + P(Ni) (giving 2.946 eV for NbNi) and D_0°(NbCo) + P(Co) (giving 3.377 eV for NbCo), although significant $d\sigma$–$s\sigma$ mixing would imply that both separated atom asymptotes contribute substantially to the bonding.

The decrease of 0.431 eV in intrinsic bond strength in moving from NbCo to NbNi reflects the addition of a second electron to the weakly antibonding δ^* orbital. It seems more likely, however, that the major effect in moving from cobalt to nickel is the decrease in the size of the 3d orbitals, which reduces the contribution of d bonding in the NbNi species. These effects are almost exactly balanced by the higher promotion energy of cobalt as compared to nickel, giving NbCo and NbNi bond dissociation energies which are identical to within 0.05 eV.

This work demonstrates that a number of distinct factors are important in determining the strength of the chemical bond in the intermetallic early–late transition metal diatomics. There is clear evidence that the late metal atom (cobalt or nickel) is promoted to the $d^n s^1$ configuration in all of the compounds that have been investigated, and the different promotion energies of cobalt *vs* nickel are reflected in the measured bond dissociation energies. In addition, the reduced size of the 3d orbitals in nickel causes the d-orbital contributions to the bond strengths of the nickel compounds to be reduced compared to those of the cobalt compounds. Thus, in moving from YNi to ZrNi and on to NbNi, one sequentially adds $d\delta^*$ electrons to the system, but this only decreases the intrinsic bond strength by 0.043 and 0.081 eV in moving from YNi to ZrNi and from ZrNi to NbNi, respectively. In contrast to this minor dependence of the intrinsic bond strength on the number of d electrons in the nickel systems, the cobalt molecules show a rather substantial dependence. The ZrCo molecule, for example, shows by far the greatest intrinsic bond strength of the mixed early–late transition metal diatomics investigated in this series, and it is also the molecule which is thought to have an electron configuration in which all of the d bonding orbitals are filled. Removing a bonding $d\delta$ electron from ZrCo to form YCo reduces the intrinsic bond strength by 0.546 eV, while adding an antibonding $d\delta^*$ electron to ZrCo to form NbCo decreases the intrinsic bond strength by 0.408 eV. Thus, the $d\delta$ and $d\delta^*$ orbitals are essentially nonbonding in the nickel compounds but contribute substantially to the bond strength in the cobalt compounds. Similar considerations apply in the intermetallic 3d compounds TiCo and VNi, where the intrinsic bond strength of TiCo exceeds that of VNi by 0.783 eV,[8] a fact which cannot be explained by the mere presence of two additional antibonding $d\delta^*$ electrons in VNi. In these compounds it is again evident that the multiple d-electron bonds in TiCo are much stronger than those in VNi, primarily due to the compact nature of the 3d orbitals in nickel (and vanadium).

V. Conclusion

The bond energies of seven diatomic transition metal molecules have been measured by the observation of an abrupt predissociation threshold in an extremely congested optical spectrum, resulting in measured values of $D_0^\circ(\mathrm{YCo}) = 2.591 \pm 0.001$ eV, $D_0^\circ(\mathrm{YNi}) = 2.904 \pm 0.001$ eV, $D_0^\circ(\mathrm{ZrCo}) = 3.137 \pm 0.001$ eV, $D_0^\circ(\mathrm{ZrNi}) = 2.861 \pm 0.001$ eV, $D_0^\circ(\mathrm{NbCo}) = 2.729 \pm 0.001$ eV, $D_0^\circ(\mathrm{NbNi}) = 2.780 \pm 0.001$ eV, and $D_0^\circ(\mathrm{Zr}_2) = 3.052 \pm 0.001$ eV. The first six of these species may be classified as early–late transition metal diatomics, in which bonding may be partially described by a Brewer–Engel model. The large bond energies obtained in these cases argue in favor of a mechanism in which s-electron density is donated to the late transition metal atom, with a concomitant back-donation of d-electron density to the d-electron deficient early transition metal atom.

The homonuclear Zr_2 molecule displays an interesting double predissociation threshold corresponding to dissociation to both the ground $4d^2 5s^2$, $^3F_2$ + $4d^2 5s^2$, $^3F_2$ and the spin–orbit excited $4d^2 5s^2$, $^3F_3$ + $4d^2 5s^2$, $^3F_2$ separated atom limits. The exact correspondence of the separation between these thresholds (570 $\pm$ 3 cm^{-1}) with the spin–orbit interval in atomic zirconium (571.41 cm^{-1}) indicates that predissociation occurs abruptly as soon as the excited molecule has sufficient energy to dissociate to a limit which generates the appropriate values of the good quantum numbers Ω, g/u, and $0^+/0^-$. The previous observation of a similar double threshold in V_2 provides strong support for assignment of the predissociation thresholds observed in the present work to actual bond dissociation energies. In addition, Zr_2 has by far the

greatest intrinsic bond strength of any of the species presently investigated. This is thought to result from the perfect size match of the 4d-orbitals on the two metal centers, combined with their significant spatial extent, which allows 4d bonds to form without difficulty.

The chemical bonding in the early–late transition metal diatomics is discussed in terms of three major factors, which combine to determine the strength of the chemical bond. First among these is the promotion energy, which is required to prepare the metal atoms for chemical bonding. In the examples considered here it appears that in all cases the cobalt or nickel atom is promoted to a $d^n s^1$ state prior to bonding. A second consideration of considerable importance is the extent of d-orbital overlap between the early and late transition metals. The compact nature of the 3d-orbitals on nickel causes the d-orbital contribution to the chemical bonding to be reduced in all of the nickel compounds studied, as compared to the corresponding cobalt compounds. Finally, the number of d-electrons available for bonding determines the occupation of the d-based bonding and antibonding orbitals, and in the cobalt-containing molecules either the addition of a $d\delta^*$ electron to ZrCo to form NbCo or the removal of a $d\delta$ electron from ZrCo to form YCo leads to a significant reduction in bond strength.

Acknowledgment. We gratefully acknowledge research support from U.S. National Science Foundation under Grant No. CHE-9215193. Acknowledgment is also made to the donors of the Petroleum Research Fund, administered by the American Chemical Society, for partial support of this research. Financial support from the Knut and Alice Wallenberg Foundation and the Swedish National Research Council (Contract No. F.FU 3867–309) is also acknowledged.

References and Notes

(1) Weltner, W., Jr.; Van Zee, R. J. *Ann. Rev. Phys. Chem.* **1984**, *35*, 291.
(2) Morse, M. D. *Chem. Rev.* **1986**, *86*, 1049.
(3) Walch, S. P.; Bauschlicher, C. W., Jr. In *Comparison of Ab Initio Quantum Chemistry with Experiment*; Bartlett, R. J., Ed.; D. Reidel: Dordrecht, 1985; p 17.
(4) Salahub, D. R. *Adv. Chem. Phys.* **1987**, *69*, 447.
(5) Bauschlicher, C. W., Jr.; Partridge, H.; Langhoff, S. R.; Rosi, M. *J. Chem. Phys.* **1991**, *95*, 1057.
(6) Doverstål, M.; Lindgren, B.; Sassenberg, U.; Arrington, C. A.; Morse, M. D. *J. Chem. Phys.* **1992**, *97*, 7087.
(7) Balasubramanian, K.; Ravimohan, Ch. *J. Chem. Phys.* **1990**, *92*, 3659.
(8) Spain, E. M.; Morse, M. D. *J. Phys. Chem.* **1992**, *96*, 2479.
(9) Morse, M. D.; Hansen, G. P.; Langridge-Smith, P. R. R.; Zheng, L.-S.; Geusic, M. E.; Michalopoulos, D. L.; Smalley, R. E. *J. Chem. Phys.* **1984**, *80*, 5400.
(10) Taylor, S.; Spain, E. M.; Morse, M. D. *J. Chem. Phys.* **1990**, *92*, 2698.
(11) Taylor, S.; Lemire, G. W.; Hamrick, Y.; Fu, Z.-W.; Morse, M. D. *J. Chem. Phys.* **1988**, *89*, 5517.
(12) Behm, J. M.; Arrington, C. A.; Morse, M. D. *J. Chem. Phys.* **1993**, *99*, 6409.
(13) Russon, L. M.; Heidecke, S. A.; Birke, M. K.; Conceicao, J.; Armentrout, P. B.; Morse, M. D. *Chem. Phys. Lett.* **1992**, *204*, 235.
(14) Russon, L. M.; Heidecke, S. A.; Birke, M. K.; Conceicao, J.; Morse, M. D.; Armentrout, P. B. *J. Chem. Phys.*, in press.
(15) Taylor, S.; Spain, E. M.; Morse, M. D. *J. Chem. Phys.* **1990**, *92*, 2710.
(16) Brewer, L. *Science* **1968**, *161*, 115. Engel, N. *Kem. Maanedsbl.* **1949**, *30*, 53, 75, 97, 105, 113. Engel, N. *Powder Metall. Bull.* **1964**, *7*, 8. Engel, N. *Am. Soc. Metals, Trans. Quart.* **1964**, *57*, 610.
(17) Fu, Z.-W.; Lemire, G. W.; Hamrick, Y.; Taylor, S.; Shui, J.-C.; Morse, M. D. *J. Chem. Phys.* **1988**, *88*, 3524.
(18) Gupta, S. K.; Gingerich, K. A. *J. Chem. Phys.* **1979**, *70*, 5350.
(19) Moore, C. E. *Nat'l Bur. Stand. (U.S.) Circ. No. 467* **1971**, Vols. I-III.
(20) Gerstenkorn, S.; Luc, P. *Atlas du Spectre d'Absorption de la Molecule d'Iode*; CRNS, Paris, 1978. Gerstenkorn, S.; Luc, P. *Rev. Phys. Appl.* **1979**, *14*, 791.
(21) Clouthier, D. J.; Karolczak, J. *Rev. Sci. Instrum.* **1990**, *61*, 1607.
(22) Lessen, D. E.; Asher, R. L.; Brucat, P. J. *Chem. Phys. Lett.* **1991**, *182*, 412.
(23) Su, C.-X.; Hales, D. A.; Armentrout, P. B. *Chem. Phys. Lett.* **1993**, *201*, 199.
(24) Herzberg, G. *Molecular Spectra and Molecular Structure I. Spectra of Diatomic Molecules*; Van Nostrand Reinhold: New York, 1950; pp 321–322.
(25) Lefebvre-Brion, H.; Field, R. W. *Perturbations in the Spectra of Diatomic Molecules*; Academic Press: Orlando, 1986, p 39.
(26) Hales, D. A.; Armentrout, P. B. *J. Cluster Science* **1990**, *1*, 127.
(27) Miedema, A. R.; Gingerich, K. A. *J. Phys. B* **1979**, *12*, 2081.
(28) Van Zee, R. J.; Weltner, W., Jr. *Chem. Phys. Lett.* **1988**, *150*, 329.
(29) Verhaegen, G.; Smoes, S.; Drowart, J. *J. Chem. Phys.* **1964**, *40*, 239.
(30) Faegri, K., Jr.; Bauschlicher, C. W., Jr. *Chem. Phys.* **1991**, *153*, 399.
(31) Shim, I.; Gingerich, K. A. *J. Chem. Phys.* **1983**, *78*, 5693.
(32) Mandich, M. L.; Halle, L. F.; Beauchamp, J. L. *J. Am. Chem. Soc.* **1984**, *106*, 4403. Elkind, J. L.; Armentrout, P. B. *J. Phys. Chem.* **1985**, *89*, 5626. Elkind, J. L.; Armentrout, P. B. *Inorg. Chem.* **1986**, *25*, 1078.
(33) Desclaux, J. P. *Atomic Data Nuclear Data Tables* **1973**, *12*, 311.
(34) Van Zee, R. J.; Weltner, W., Jr. *Chem. Phys. Lett.* **1984**, *107*, 173.
(35) Bishea, G. A.; Marak, N.; Morse, M. D. *J. Chem. Phys.* **1991**, *95*, 5618.
(36) Van Zee, R. J.; Weltner, W., Jr. *High Temp. Sci.* **1984**, *17*, 181.
(37) Spain, E. M.; Morse, M. D. *J. Chem. Phys.* **1992**, *97*, 4641.
(38) Cheeseman, M.; Van Zee, R. J.; Weltner, W., Jr. *High Temp. Sci.* **1988**, *25*, 143.
(39) Morse, M. D. *Adv. Metal Semicond. Clusters* **1993**, *1*, 83.
(40) Ran, Q.; Schmude, R. W., Jr.; Gingerich, K. A.; Wilhite, D. W.; Kingcade, J. E., Jr. *J. Phys. Chem.* **1993**, *97*, 8535.